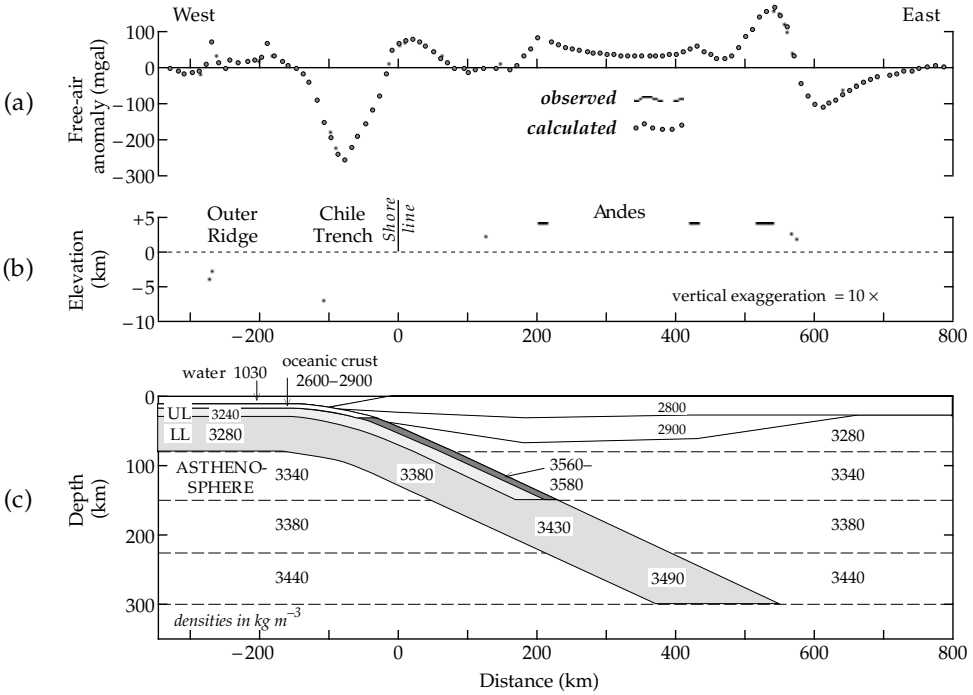

Fig. 2.62 Observed and computed free-air gravity anomalies across a subduction zone. The density model for the computed anomaly is based on seismic, thermal and petrological data. The profile crosses the Chile trench and Andes mountains at 23°S (after Grow and Bowin, 1975).

beneath the ridge, melts and accumulates in a shallow magma chamber within the oceanic crust.

2.6.4.4 Gravity anomalies at subduction zones

Subduction zones are found primarily at continental margins and island arcs. Elongate, narrow and intense isostatic and free-air gravity anomalies have long been associated with island arcs. The relationship of gravity to the structure of a subduction zone is illustrated by the free-air anomaly across the Chile trench at 23°S (Fig. 2.62). Seismic refraction data define the thicknesses of the oceanic and continental crust. Thermal and petrological data are integrated to give a density model for the structure of the mantle and the subducting lithosphere.

The continental crust is about 65 km thick beneath the Andes mountains, and gives large negative Bouguer anomalies. The free-air gravity anomaly over the Andes is positive, averaging about + 50 mgal over the 4 km high plateau. Even stronger anomalies up to + 100 mgal are seen over the east and west boundaries of the Andes. This is largely due to the edge effect of the low-density Andean crustal block (see Fig. 2.44b and Section 2.5.6).

A strong positive free-air anomaly of about + 70 mgal lies between the Andes and the shore-line of the Pacific ocean. This anomaly is due to the subduction of the Nazca plate beneath South America. The descending slab is old and cool. Subduction exposes it to higher temperatures and pressures, but the slab descends faster than it can be heated up. The increase in density accompanying greater depth and pressure outweighs the decrease in density due to hotter temperatures. There is a positive density contrast between the subducting lithosphere and the surrounding mantle. Also, petrological changes accompanying the subduction result in mass excesses. Peridotite in the upper lithosphere changes phase from plagioclase-type to the higher-density garnet-type. When oceanic crust is subducted to depths of 30–80 km, basalt changes phase to eclogite, which has a higher density (3560–3580 kg m^{-3}) than upper mantle rocks. These effects combine to produce the positive free-air anomaly.

The Chile trench is more than 2.5 km deeper than the ocean basin to the west. The sediments flooring the trench have low density. The mass deficiency of the water and sediments in the trench cause a strong negative free-air anomaly, which parallels the trench and has an amplitude greater than −250 mgal. A small positive anomaly of about + 20 mgal is present about 100 km seaward of the trench axis. This anomaly is evident also in the mean level of the ocean surface as mapped by SEASAT (Fig. 2.28), which shows that the mean sea surface is raised in front of deep ocean trenches. This is due to upward flexure of the lithosphere before its downward plunge into the subduction zone. The flexure elevates higher-density mantle rocks and thereby causes the small positive free-air anomaly.

2.7 ISOSTASY

2.7.1 The discovery of isostasy

Newton formulated the law of universal gravitation in 1687 and confirmed it with Kepler's laws of planetary motion. However, in the seventeenth and eighteenth centuries the law could not be used to calculate the mass or mean density of the Earth, because the value of the gravitational constant was not yet known (it was first determined by Cavendish in 1798). Meanwhile, eighteenth century scientists attempted to estimate the mean density of the Earth

by various means. They involved comparing the attraction of the Earth with that of a suitable mountain, which could be calculated. Inconsistent results were obtained.

During the French expedition to Peru in 1737–1740, Pierre Bouguer measured gravity with a pendulum at different altitudes, applying the elevation correction term which now bears his name. If the density of crustal rocks is ρ and the mean density of the Earth is ρ_0, the ratio of the Bouguer-plate correction (see Section 2.5.4.3) for elevation h to mean gravity for a spherical Earth of radius R is

$$\frac{\Delta g_{\mathrm{BP}}}{g} = \frac{2\pi G\rho h}{\frac{4}{3}\pi G\rho_0 R} = \frac{3}{2}\left(\frac{\rho}{\rho_0}\right)\left(\frac{h}{R}\right) \tag{2.103}$$

From the results he obtained near Quito, Bouguer estimated that the mean density of the Earth was about 4.5 times the density of crustal rocks.

The main method employed by Bouguer to determine the Earth's mean density consisted of measuring the deflection of the plumb-line (vertical direction) by the mass of a nearby mountain (Fig. 2.63). Suppose the elevation of a known star is measured relative to the local vertical direction at points N and S on the same meridian. The elevations should be α_{N} and α_{S}, respectively. Their sum is α, the angle subtended at the center of the Earth by the radii to N and S, which corresponds to the difference in latitude. If N and S lie on opposite sides of a large mountain, the plumb-line at each station is deflected by the attraction of the mountain. The measured elevations of the star are β_{N} and β_{S}, respectively, and their sum is β. The local vertical directions now intersect at the point D instead of at the center of the (assumed spherical) Earth. The difference $\delta = \beta - \alpha$ is the sum of the deviations of the vertical direction caused by the mass of the mountain.

The horizontal attraction f of the mountain can be calculated from its shape and density, with a method that resembles the computation of the topographic correction in the reduction of gravity measurements. Dividing the mountain into vertical cylindrical elements, the horizontal attraction of each element is calculated and its component ($G\rho h_i$) towards the center of mass of the mountain is found. Summing up the effects of all the cylindrical elements in the mountain gives the horizontal attraction f towards its center of mass. Comparing f with mean gravity g, we then write

$$\tan\delta = \frac{f}{g} = \frac{G\rho\sum_i h_i}{\frac{4}{3}\pi G\rho_0 R} = \frac{\sum_i h_i}{\frac{4}{3}\pi R}\left(\frac{\rho}{\rho_0}\right) \tag{2.104}$$

For very small angles, $\tan\delta$ is equal to δ, and so the deflection of the vertical is proportional to the ratio ρ/ρ_0 of the mean densities of the mountain and the Earth. Bouguer measured the deflection of the vertical caused by Mt. Chimborazo (6272 m), Ecuador's highest mountain. His results gave a ratio ρ/ρ_0 of around 12, which is unrealistically large and quite different from the values he had obtained near Quito. The erroneous result indicated that the deflection of the vertical caused by the mountain was much too small for its estimated mass.

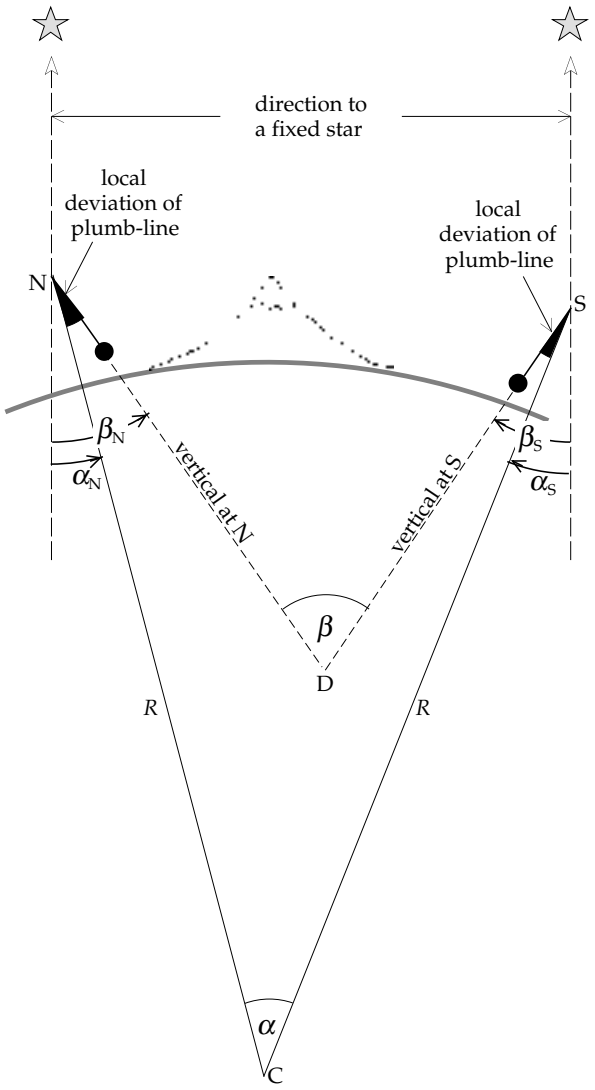

Fig. 2.63 Deviations of the local plumb-line at N and S on opposite sides of a large mountain cause the local vertical directions to intersect at the point D instead of at the center of the Earth.

In 1774 Bouguer's Chimborazo experiment was repeated in Scotland by Neville Maskelyne on behalf of the Royal Society of London. Measurements of the elevations of stars were made on the north and south flanks of Mt. Schiehallion at sites that differed in latitude by 42.9″ of arc. The observed angle between the plumb-lines was 54.6″. The analysis gave a ratio ρ/ρ_0 equal to 1.79, suggesting a mean density for the Earth of 4500 kg m^{-3}. This was more realistic than Bouguer's result, which still needed explanation.

Further results accumulated in the first half of the nineteenth century. From 1806 to 1843 the English geodesist George Everest carried out triangulation surveys in India. He measured by triangulation the separation of a site at Kalianpur on the Indo-Ganges plain from a site at Kaliana in the foothills of the Himalayas. The distance differed substantially from the separation of the sites

computed from the elevations of stars, as in Fig. 2.63. The discrepancy of 5.23″ of arc (162 m) was attributed to deflection of the plumb-line by the mass of the Himalayas. This would affect the astronomic determination but not the triangulation measurement. In 1855 J. H. Pratt computed the minimum deflection of the plumb-line that might be caused by the mass of the Himalayas and found that it should be 15.89″ of arc, about three times larger than the observed deflection. Evidently the attraction of the mountain range on the plumb-line was not as large as it should be.

The anomalous deflections of the vertical were first understood in the middle of the nineteenth century, when it was realized that there are regions beneath mountains – "root-zones" – in which rocks have a lower density than expected. The deflection of a plumb-line is not caused only by the horizontal attraction of the visible part of a mountain. The deficiency of mass at depth beneath the mountain means that the "hidden part" exerts a reduced lateral attraction, which partly offsets the effect of the mountain and diminishes the deflection of the vertical. In 1889 C. E. Dutton referred to the compensation of a topographic load by a less-dense subsurface structure as *isostasy*.

2.7.2 Models of isostasy

Separate explanations of the anomalous plumb-line deflections were put forward by G. B. Airy in 1855 and J. H. Pratt in 1859. Airy was the Astronomer Royal and director of the Greenwich Observatory. Pratt was an archdeacon of the Anglican church at Calcutta, India, and a devoted scientist. Their hypotheses have in common the compensation of the extra mass of a mountain above sea-level by a less-dense region (or root) below sea-level, but they differ in the way the compensation is achieved. In the Airy model, when isostatic compensation is complete, the mass deficiency of the root equals the excess load on the surface. At and below a certain *compensation depth* the pressure exerted by all overlying vertical columns of crustal material is then equal. The pressure is then *hydrostatic*, as if the interior acted like a fluid. Hence, isostatic compensation is equivalent to applying Archimedes' principle to the uppermost layers of the Earth.

The Pratt and Airy models achieve compensation locally by equalization of the pressure below vertical columns under a topographic load. The models were very successful and became widely used by geodesists, who developed them further. In 1909–1910, J. F. Hayford in the United States derived a mathematical model to describe the Pratt hypothesis. As a result, this theory of isostasy is often called the Pratt–Hayford scheme of compensation. Between 1924 and 1938 W. A. Heiskanen derived sets of tables for calculating isostatic corrections based on the Airy model. This concept of isostatic compensation has since been referred to as the Airy–Heiskanen scheme.

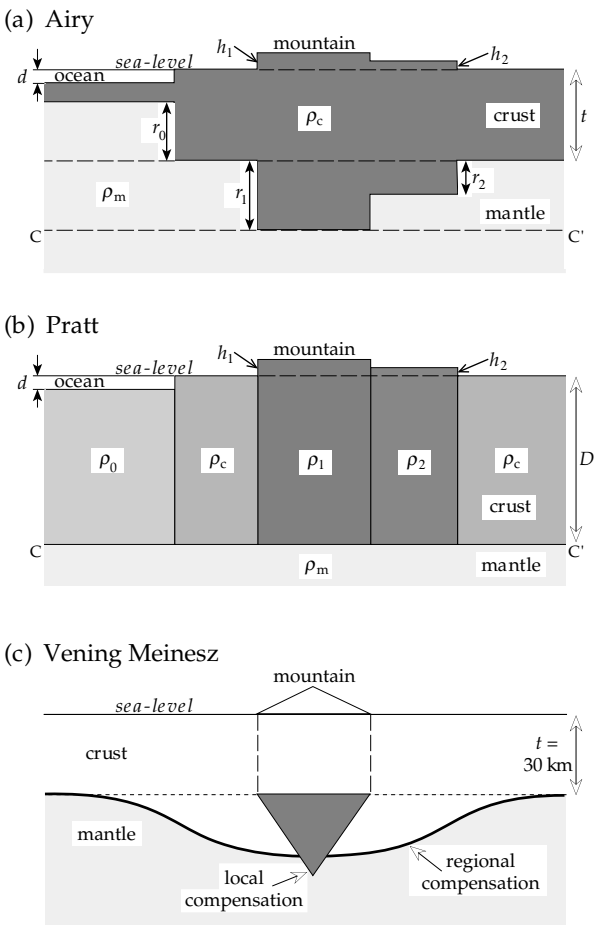

Fig. 2.64 Local isostatic compensation according to (a) the Airy–Heiskanen model and (b) the Pratt–Hayford model; (c) regional compensation according to the elastic plate model of Vening Meinesz.

It became apparent that both models had serious deficiencies in situations that required compensation over a larger region. In 1931 F. A. Vening Meinesz, a Dutch geophysicist, proposed a third model, in which the crust acts as an elastic plate. As in the other models, the crust floats buoyantly on a substratum, but its inherent rigidity spreads topographic loads over a broader region.

2.7.2.1 The Airy–Heiskanen model

According to the Airy–Heiskanen model of isostatic compensation (Fig. 2.64a) an upper layer of the Earth "floats" on a denser magma-like substratum, just as icebergs float in water. The upper layer is equated with the crust and the substratum with the mantle. The height of a mountain above sea-level is much less than the thickness of the crust underneath it, just as the visible tip of an iceberg is much smaller than the subsurface part. The densities of the crust and mantle are assumed to be constant; the thickness of the root-zone varies in proportion to the elevation of the topography.

The analogy to an iceberg is not exact, because under land at sea-level the "normal" crust is already about 30–35 km thick; the compensating root-zone of a

mountain lies below this depth. Oceanic crust is only about 10 km thick, thinner than the "normal" crust. The mantle between the base of the oceanic crust and the normal crustal depth is sometimes called the *anti-root* of the ocean basin.

The Airy–Heiskanen model assumes local isostatic compensation, i.e., the root-zone of a mountain lies directly under it. Isostasy is assumed to be complete, so that hydrostatic equilibrium exists at the compensation depth, which is equivalent to the base of the deepest mountain root. The pressure at this level is due to the weight of the rock material in the overlying vertical column (of basal area one square meter) extending to the Earth's surface. The vertical column for the mountain of height h_1 in Fig. 2.64a contains only crustal rocks of density ρ_c. The pressure at CC′ due to the mountain, "normal" crust of thickness t, and a root-zone of thickness r_1 amounts to $(h_1 + t + r_1)\rho_c$. The vertical column below the "normal" crust contains a thickness t of crustal rocks and thickness r_1 of mantle rocks; it exerts a pressure of $(t\rho_c + r_1\rho_m)$. For hydrostatic equilibrium the pressures are equal. Equating, and noting that each expression contains the term $t\rho_c$, we get

$$r_1 = \frac{\rho_c}{\rho_m - \rho_c} h_1 \tag{2.105}$$

with a similar expression for the root of depth r_2 under the hill of height h_2. The thickness r_0 of the anti-root of the oceanic crust under an ocean basin of water depth d and density ρ_w is given by

$$r_0 = \frac{\rho_c - \rho_w}{\rho_m - \rho_c} d \tag{2.106}$$

The Airy–Heiskanen model assumes an upper layer of constant density floating on a more dense substratum. It has root-zones of variable thickness proportional to the overlying topography. This scenario agrees broadly with seismic evidence for the thickness of the Earth's crust (see Section 3.7). The continental crust is much thicker than the oceanic crust. Its thickness is very variable, being largest below mountain chains, although the greatest thickness is not always under the highest topography. Airy-type compensation suggests hydrostatic balance between the crust and the mantle.

2.7.2.2 The Pratt–Hayford model

The Pratt–Hayford isostatic model incorporates an outer layer of the Earth that rests on a weak magmatic substratum. Differential expansion of the material in vertical columns of the outer layer accounts for the surface topography, so that the higher the column above a common base the lower the mean density of rocks in it. The vertical columns have constant density from the surface to their base at depth D below sea-level (Fig. 2.64b). If the rock beneath a mountain of height h_i ($i = 1, 2,...$) has density ρ_i, the pressure at CC′ is $\rho_i(h_i + D)$. Beneath a continental region at sea-level the pressure of the rock column of density ρ_c is $\rho_c D$. Under an ocean basin the pressure at CC′ is due to water of depth d and density ρ_w on top of a rock column of thickness $(D - d)$ and density ρ_0; it is equal to $\rho_w d + \rho_0(D - d)$. Equating these pressures, we get

$$\rho_i = \frac{D}{h_i + D}\rho_c \tag{2.107}$$

for the density below a topographic elevation h_i, and

$$\rho_0 = \frac{\rho_c D - \rho_w d}{D - d} \tag{2.108}$$

for the density under an oceanic basin of depth d. The compensation depth D is about 100 km.

The Pratt–Hayford and Airy–Heiskanen models represent *local isostatic compensation*, in which each column exerts an equal pressure at the compensation level. At the time these models were proposed very little was yet known about the internal structure of the Earth. This was only deciphered after the development of seismology in the late nineteenth and early twentieth century. Each model is idealized, both with regard to the density distributions and the behavior of Earth materials. For example, the upper layer is assumed to offer no resistance to shear stresses arising from vertical adjustments between adjacent columns. Yet the layer has sufficient strength to resist stresses due to horizontal differences in density. It is implausible that small topographic features require compensation at large depths; more likely, they are entirely supported by the strength of the Earth's crust.

2.7.2.3 Vening Meinesz elastic plate model

In the 1920s F. A. Vening Meinesz made extensive gravity surveys at sea. His measurements were made in a submarine to avoid the disturbances of wave motions. He studied the relationship between topography and gravity anomalies over prominent topographic features, such as the deep sea trenches and island arcs in southeastern Asia, and concluded that isostatic compensation is often not entirely local. In 1931 he proposed a model of *regional isostatic compensation* which, like the Pratt–Hayford and Airy–Heiskanen models, envisages a light upper layer that floats on a denser fluid substratum. However, in the Vening Meinesz model the upper layer behaves like an elastic plate overlying a weak fluid. The strength of the plate distributes the load of a surface feature (e.g., an island or seamount) over a horizontal distance wider than the feature (Fig. 2.64c). The topographic load bends the plate downward into the fluid substratum, which is pushed aside. The buoyancy of the displaced fluid forces it upward, giving support to the bent plate at distances well away from the central depression. The bending of the plate which accounts for the regional compensation in the Vening Meinesz model depends on the elastic properties of the lithosphere.

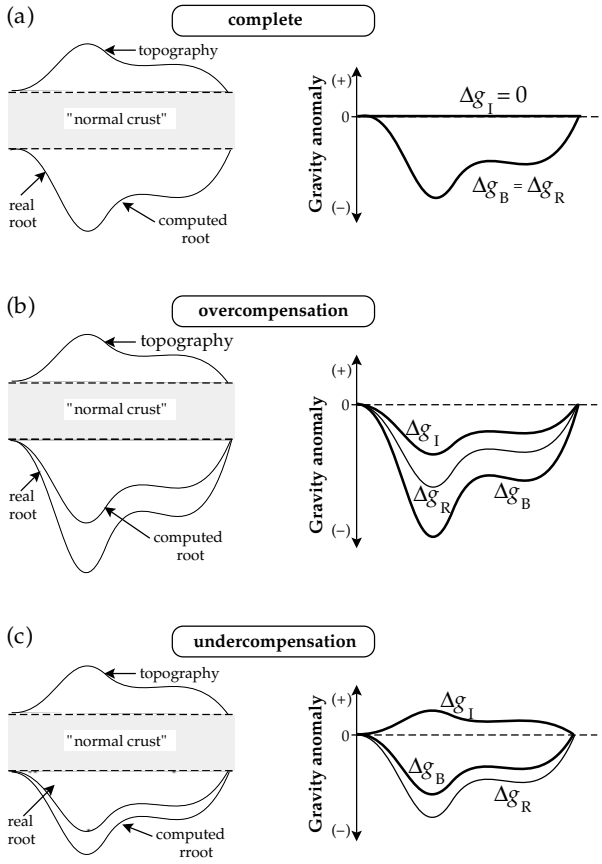

Fig. 2.65 Explanation of the isostatic gravity anomaly (Δg_I) as the difference between the Bouguer gravity anomaly (Δg_B) and the computed anomaly (Δg_R) of the root-zone estimated from the topography for (a) complete isostatic compensation, (b) isostatic overcompensation and (c) isostatic undercompensation.

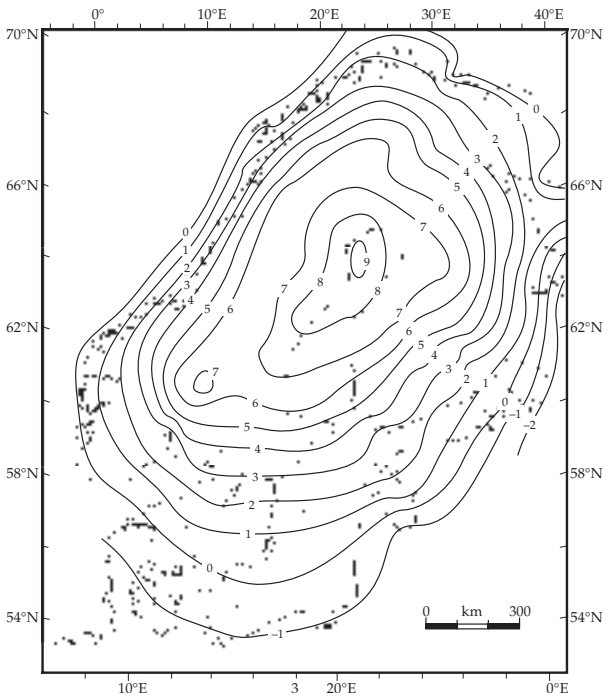

Fig. 2.66 Fennoscandian rates of vertical crustal movement (in mm yr^{-1}) relative to mean sea-level. Positive rates correspond to uplift, negative rates to subsidence (after Kakkuri, 1992).

2.7.3 Isostatic compensation and vertical crustal movements

In the Pratt–Hayford and Airy–Heiskanen models the lighter crust floats freely on the denser mantle. The system is in hydrostatic equilibrium, and local isostatic compensation is a simple application of Archimedes' principle. A "normal" crustal thickness for sea-level coastal regions is assumed (usually 30–35 km) and the additional depths of the root-zones below this level are exactly proportional to the elevations of the topography above sea-level. The topography is then *completely compensated* (Fig. 2.65a). However, isostatic compensation is often incomplete. The geodynamic imbalance leads to vertical crustal movements.

Mountains are subject to erosion, which can disturb isostatic compensation. If the eroded mountains are no longer high enough to justify their deep root-zones, the topography is isostatically *overcompensated* (Fig. 2.65b). Buoyancy forces are created, just as when a wooden block floating in water is pressed downward by a finger; the underwater part becomes too large in proportion to the amount above the surface. If the finger pressure is removed, the block rebounds in order to restore hydrostatic equilibrium. Similarly, the buoyancy forces that result from overcompensation of mountainous topography cause vertical *uplift*. The opposite scenario is also possible. When the visible topography has roots that are too small, the topography is isostatically *undercompensated* (Fig. 2.65c). This situation can result, for example, when tectonic forces thrust crustal blocks on top of each other. Hydrostatic equilibrium is now achieved by *subsidence* of the uplifted region.

The most striking and best-observed examples of vertical crustal movements due to isostatic imbalance are related to the phenomenon of glacial rebound observed in northern Canada and in Fennoscandia. During the latest ice-age these regions were covered by a thick ice-cap. The weight of ice depressed the underlying crust. Subsequently melting of the ice-cap removed the extra load on the crust, and it has since been rebounding. At stations on the Fennoscandian shield, modern tide-gauge observations and precision levelling surveys made years apart allow the present uplift rates to be calculated (Fig. 2.66). The contour lines of equal uplift rate are inexact over large areas due to the incompleteness of data from inaccessible regions. Nevertheless, the general pattern of glacial rebound is clearly recognizable, with uplift rates of up to 8 mm yr^{-1}.

2.7.4 Isostatic gravity anomalies

The different degrees of isostatic compensation find expression in gravity anomalies. As explained in Section 2.5.6 the free-air gravity anomaly Δg_F is small near the center of a large region that is isostatically compensated; the Bouguer anomaly Δg_B is strongly negative. Assuming complete isostatic compensation, the size and shape of the root-zone

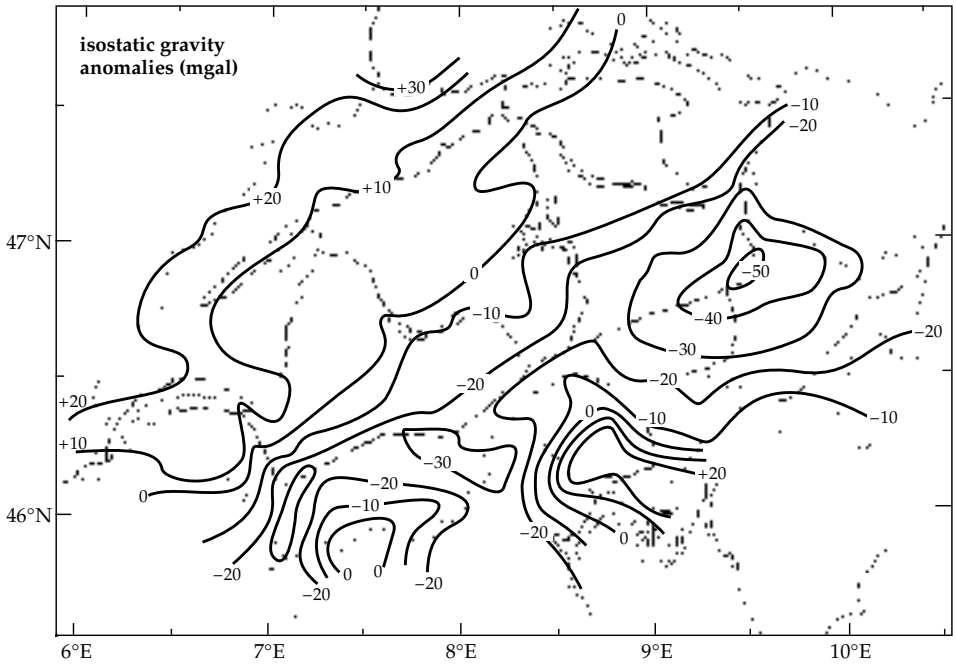

Fig. 2.67 Isostatic gravity anomalies in Switzerland (after Klingelé and Kissling, 1982), based on the national gravity map (Klingelé and Olivier, 1980), corrected for the effects of the Molasse basin and the Ivrea body.

can be determined from the elevations of the topography. With a suitable density contrast the gravity anomaly Δg_R of the modelled root-zone can be calculated; because the root-zone has lower density than adjacent mantle rocks Δg_R is also negative. The *isostatic gravity anomaly* Δg_I is defined as the difference between the Bouguer gravity anomaly and the computed anomaly of the root-zone, i.e.,

$$\Delta g_I = \Delta g_B - \Delta g_R \tag{2.109}$$

Examples of the isostatic gravity anomaly for the three types of isostatic compensation are shown schematically in Fig. 2.65. When isostatic compensation is complete, the topography is in hydrostatic equilibrium with its root-zone. Both Δg_B and Δg_R are negative but equal; consequently, the isostatic anomaly is everywhere zero ($\Delta g_I = 0$). In the case of overcompensation the eroded topography suggests a root-zone that is smaller than the real root-zone. The Bouguer anomaly is caused by the larger real root, so Δg_B is numerically larger than ΔgR. Subtracting the smaller negative anomaly of the computed root-zone leaves a negative isostatic anomaly ($\Delta g_I < 0$). On the other hand, with undercompensation the topography suggests a root-zone that is larger than the real root-zone. The Bouguer anomaly is caused by the smaller real root, so Δg_B is numerically smaller than Δg_R. Subtracting the larger negative anomaly of the root-zone leaves a positive isostatic anomaly ($\Delta g_I > 0$).

A national gravity survey of Switzerland carried out in the 1970s gave a high-quality map of Bouguer gravity anomalies (see Fig. 2.58). Seismic data gave representative parameters for the Central European crust and mantle: a crustal thickness of 32 km without topography, and mean densities of 2670 kg m^{-3} for the topography, 2810 kg m^{-3} for the crust and 3310 kg m^{-3} for the mantle. Using the Airy–Heiskanen model of compensation, a map of isostatic gravity anomalies in Switzerland was derived (Fig. 2.67) after correcting the gravity map for the effects of low-density sediments in the Molasse Basin north of the Alps and high-density material in the anomalous Ivrea body in the south.

The pattern of isostatic anomalies reflects the different structures beneath the Jura mountains, which do not have a prominent root-zone, and the Alps, which have a low-density root that extends to more than 55 km depth in places. The dominant ENE–WSW trend of the isostatic gravity anomaly contour lines is roughly parallel to the trends of the mountain chains. In the northwest, near the Jura mountains, positive isostatic anomalies exceed 20 mgal. In the Alps isostatic anomalies are mainly negative, reaching more than −50 mgal in the east.

A computation based on the Vening Meinesz model gave an almost identical isostatic anomaly map. The agreement of maps based on the different concepts of isostasy is somewhat surprising. It may imply that vertical crustal columns are not free to adjust relative to one another without friction as assumed in the Airy–Heiskanen model. The friction is thought to result from horizontal compressive stresses in the Alps, which are active in the on-going mountain-building process.

Comparison of the isostatic anomaly map with one of recent vertical crustal movements (Fig. 2.68) illustrates the relevance of isostatic gravity anomalies for tectonic interpretation. Precise levelling surveys have been carried out since the early 1900s along major valleys transecting and parallel to the mountainous topography of Switzerland. Relative rates of uplift or subsidence are computed from the differences between repeated surveys. The results have not been tied to absolute tide-gauge observations and so are relative to a base station at Aarburg in the canton of Aargau, in the northeast.

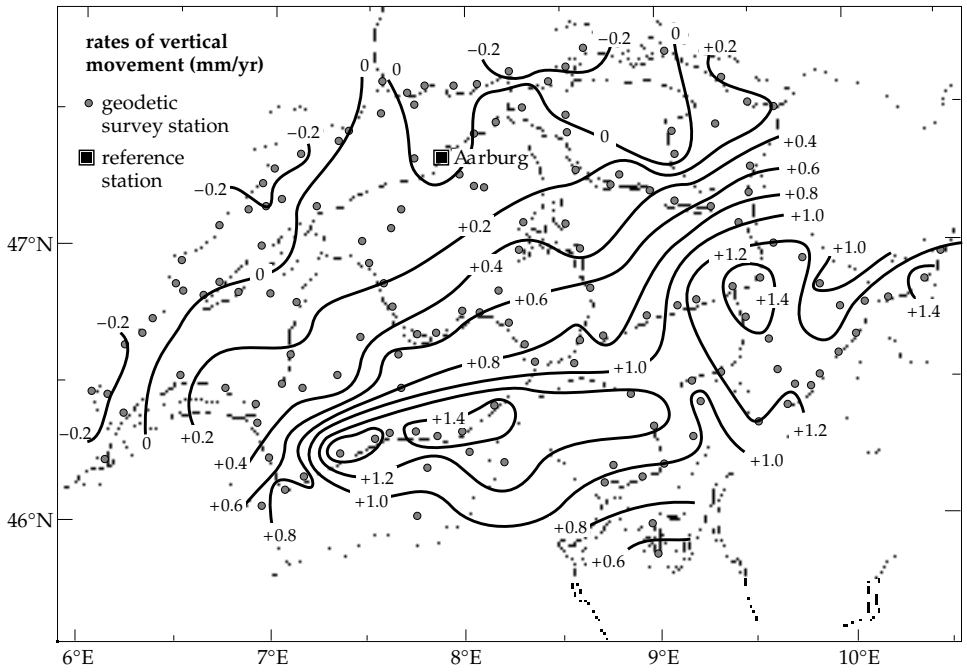

Fig. 2.68 Rates of vertical crustal motion in Switzerland deduced from repeated precise levelling. Broken contour lines indicate areas in which geodetic data are absent or insufficient. Positive rates correspond to uplift, negative rates to subsidence (data source: Gubler, 1991).

The rates of relative vertical movement in northeastern Switzerland are smaller than the confidence limits on the data and may not be significant, but the general tendency suggests subsidence. This region is characterized by mainly positive isostatic anomalies. The rates of vertical movement in the southern part of Switzerland exceed the noise level of the measurements and are significant. The most notable characteristic of the recent crustal motions is vertical uplift of the Alpine part of Switzerland relative to the central plateau and Jura mountains. The Alpine uplift rates are up to 1.5 mm yr^{-1}, considerably smaller than the rates observed in Fennoscandia. The most rapid uplift rates are observed in the region where isostatic anomalies are negative. The constant erosion of the mountain topography relieves the crustal load and the isostatic response is uplift. However, the interpretation is complicated by the fact that compressive stresses throughout the Alpine region acting on deep-reaching faults can produce non-isostatic uplift of the surface. The separation of isostatic and non-isostatic vertical crustal movements in the Alps will require detailed and exact information about the structure of the lithosphere and asthenosphere in this region.

2.8 RHEOLOGY

2.8.1 Brittle and ductile deformation

Rheology is the science of the deformation and flow of solid materials. This definition appears at first sight to contradict itself. A solid is made up of particles that cohere to each other; it is rigid and resists a change of shape. A fluid has no rigidity; its particles can move about comparatively freely. So how can a solid flow? In fact, the way in which a solid reacts to stress depends on how large the stress is and the length of time for which it is applied. Provided the applied stress does not exceed the yield stress (or elastic limit) the short-term behavior is elastic. This means that any deformation caused by the stress is completely recoverable when the stress is removed, leaving no permanent change in shape. However, if the applied stress exceeds the yield stress, the solid may experience either brittle or ductile deformation.

Brittle deformation consists of rupture without other distortion. This is an abrupt process that causes faulting in rocks and earthquakes, accompanied by the release of elastic energy in the form of seismic waves. Brittle fracture occurs at much lower stresses than the intrinsic strength of a crystal lattice. This is attributed to the presence of cracks, which modify the local internal stress field in the crystal. Fracture occurs under either extension or shear. Extensional fracture occurs on a plane at right angles to the direction of maximum tension. Shear fracture occurs under compression on one of two complementary planes which, reflecting the influence of internal friction, are inclined at an angle of less than 45° (typically about 30°) to the maximum principal compression. Brittle deformation is the main mechanism in tectonic processes that involve the uppermost 5–10 km of the lithosphere.

Ductile deformation is a slow process in which a solid acquires strain (i.e., it changes shape) over a long period of time. A material may react differently to a stress that is applied briefly than to a stress of long duration. If it experiences a large stress for a long period of time a solid can slowly and permanently change shape. The time-dependent deformation is called plastic flow and the capacity of the solid to flow is called its *ductility*. The ductility of a solid above its yield stress depends on temperature and confining pressure, and materials that are brittle under ordinary conditions may be ductile at high temperature and pressure. The behavior of rocks and minerals in